Mesoporous Materials

DOI: 10.1002/anie.200906648

Self-Assembled TiO_2 Nanocrystal Clusters for Selective Enrichment of Intact Phosphorylated Proteins**

*Zhenda Lu, Miaomiao Ye, Ni Li, Wenwan Zhong, and Yadong Yin**

Mesoporous oxides have been used for selective separation and adsorption of biomolecules.[1–11] Inorganic oxide materials such as silica can be synthesized into highly ordered mesoporous structures featuring high in-pore surface areas, narrow pore size distributions, adjustable pore sizes, and modifiable surface properties.[10,12–15] Such unique properties favor the selective enrichment of proteins or peptides based on the size-exclusion mechanism. Classic mesoporous silica structures with narrow pore size distributions, such as MCM-41 and SBA-15, have been used to selectively enrich peptides from human plasma and exclude other proteins according to an accurate molecular weight (MW) cutoff.[2–9] However, this type of enrichment method is limited mainly to silica and alumina because currently it is still difficult to extend broadly the surfactant-templating method to the synthesis of mesoporous structures of many other oxides in a convenient, controllable, and scalable manner (although the literature does contain some relevant procedures[16–18]). The limited choice of materials makes it difficult to further enhance the selectivity by taking advantage of both the size-exclusion effect and the specific binding between many oxides and proteins or peptides.

Herein, we propose a general strategy for the fabrication of novel porous nanostructured materials for the efficient separation of biomolecules such as proteins, peptides, and DNA. Briefly, nanoparticles of various nanostructured materials with uniform sizes and shapes are firstly synthesized and then self-assembled into three-dimensional submicrometer clusters containing uniform mesoscale pores. Thanks to rapid progress in colloidal nanostructure synthesis, a great number of materials can now be routinely produced in the form of nanoparticles with excellent control over size, shape, and surface properties,[19–22] making it possible to utilize specific material–protein/peptide interactions to enhance the selectivity in protein/peptide enrichment.[23,24] Additionally, size exclusion can also be achieved by controlling the dimensions of the pores produced by the packing of constituent nanoparticles,[25,26] allowing selective enrichment of biomolecules based on their sizes. The outer surface of each cluster can be made highly hydrophilic, so that nonspecific binding of many hydrophobic proteins/peptides can be avoided. The self-assembly process also brings the convenience of incorporation of multiple components into the clusters to further facilitate separation and detection. For example, the incorporation of fluorescent nanocrystals, such as quantum dots, during the assembly process may produce multifunctional microspheres that are able not only to selectively enrich but also to easily identify the targeted biomolecules. Also, adding superparamagnetic iron oxide nanocrystals to the clusters allows their efficient removal from the analyte solution after selective adsorption by using an external magnetic field.

As an example, we report herein the fabrication of mesoporous TiO_2 nanocrystal clusters and demonstrate their use for selective enrichment of intact phosphorylated proteins from complex biological samples by taking advantage of both the specific affinity offered by the metal oxide and the size-exclusion mechanism enabled by the mesoporous structure. The efficient separation and accurate analysis of phosphorylated proteins are highly demanded in biomedical applications because phosphorylation of proteins is a key event in most cellular processes, including signal transduction, gene expression, cell cycle, cytoskeletal regulation, and apoptosis.[27,28] The combination of peptide mapping by matrix-assisted laser desorption/ionization time-of-flight mass spectrometry (MALDI–TOF MS) with the methods of phosphopeptide enrichment represents an efficient tool for the characterization of the phosphorylated proteins after digestion. The most widely used approaches for specific enrichment of phosphopeptides are immobilized metal affinity chromatography (IMAC) and metal oxide affinity chromatography (MOAC).[23,29–32] In IMAC, phosphopeptides can be selectively retained because of the affinity of metal ions for the phosphate groups, whereas in MOAC, the specific adsorption results from bridging bidentate bindings formed between the phosphate anions and the surface of a metal oxide, such as TiO_2, ZrO_2, Fe_2O_3, and Al_2O_3.[33] However, these techniques can provide information about the original phosphorylated proteins only indirectly, and direct enrichment of phosphorylated proteins by IMAC or MOAC is rarely reported because of the low adsorption efficiency and significant losses of phosphorylated proteins during the washing steps.[34,35] Therefore, despite the intense interest in studying phosphorylation events, the direct enrichment of intact phosphorylated proteins remains a technical challenge. In this Communication, we describe the selective enrichment of phosphorylated proteins from protein mixtures by using mesoporous colloids of TiO_2 fabricated through self-assembly

[*] Z. Lu, M. Ye, N. Li, Prof. W. Zhong, Prof. Y. Yin
Department of Chemistry, University of California
Riverside, CA 92521 (USA)
Fax: (+1) 951-827-4713
E-mail: yadong.yin@ucr.edu
Homepage: http://faculty.ucr.edu/~yadongy/

[**] Y.Y. thanks the University of California, Riverside for start-up funds. Acknowledgement is also given to the Donors of the Petroleum Research Fund, administered by the American Chemical Society, for support of this research. Y.Y. is a Cottrell Scholar of Research Corporation for Science Advancement.

Supporting information for this article is available on the WWW under http://dx.doi.org/10.1002/anie.200906648.

of corresponding nanocrystals. The unique properties of the porous TiO_2 structures, including high specific surface area, narrow pore size distribution, adjustable pore size, low nonspecific adsorption, and great water dispersity, make them ideal adsorbents for pretreatment and enrichment of phosphorylated proteins for phosphoproteome analysis.

Clusters of densely packed TiO_2 nanocrystals were prepared by using oil-in-water emulsion droplets as templates.[36] As shown in Scheme 1, nanocrystals confined in an oil droplet were self-assembled into spherical clusters upon evaporation of the low-boiling-point solvent (the "oil"). The clusters were coated with a silica layer by a modified sol–gel process[37] and then calcined at 500 °C for 2 h in air to remove the organic ligands and enhance the mechanical stability. The silica layers were then etched away in a dilute solution of NaOH (see the Supporting Information). After washing, the clusters can remain dispersed in water with no sign of aggregation or sedimentation for several days. Zeta potential analysis showed a value of −15 mV for as-prepared clusters dispersed in water, in contrast to −3 mV for solid TiO_2 microspheres or simple aggregations of TiO_2 nanocrystals that were pretreated at high temperature in a similar way. Solid TiO_2 spheres with an average diameter of around 200 nm, which were prepared by using a sol–gel process and calcined at 500 °C for 2 h in air (see the Supporting Information), were included in measurements for comparison. It is believed that the silica coating and etching processes leave a high density of hydroxy groups on the cluster surface and subsequently enhance the surface charge and water dispersity of the clusters. As described below, the relatively high surface charge may also help to lower the nonspecific adsorption of proteins, thus increasing the selectivity of enrichment. Therefore, the silica coating and removal are important steps that not only prevent the clusters from aggregating during heating but also help to improve their surface charge and water dispersibility. X-ray diffraction measurements confirmed that the grain size of the TiO_2 nanocrystals increased only slightly after calcination (from 4.6 to 5.2 nm in a typical example shown in the Supporting Information), which may be due to the ripening process or to nanocrystal fusion at a high temperature.

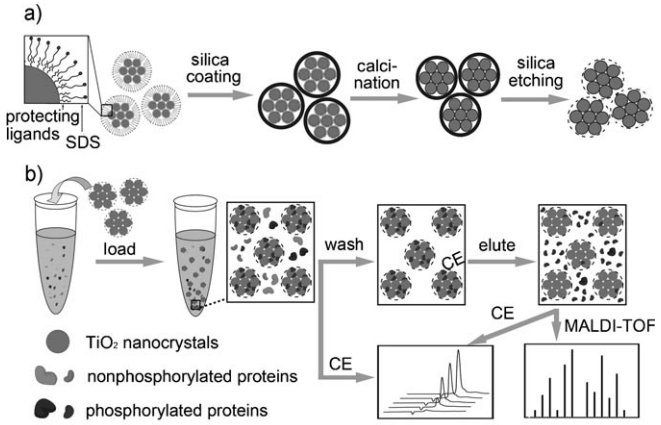

Scheme 1. Illustration of a) the procedure for the fabrication of the mesoporous TiO_2 nanocrystal clusters and b) the selective enrichment process of phosphorylated proteins using these TiO_2 clusters.

The self-assembly approach allows facile control over the pore dimensions by changing the size, shape, or composition of the nanocrystal building blocks. For comparison, we fabricated three samples of clusters by assembling TiO_2 nanodots and nanorods: NCC1 from 5.1 nm nanodots, NCC2 from 6.6 nm nanodots, and NCC3 from 3.0 nm × 28.1 nm nanorods. Representative transmission electron microscopy (TEM) images of clusters and corresponding primary TiO_2 nanocrystals are shown in Figure 1. One can easily observe the porous nature of the clusters by carefully inspecting the enlarged images in the insets. Sample NCC3, which is composed of TiO_2 nanorods, has the largest pores. N_2 adsorption–desorption isotherms were used to examine the porous structures (Figure 1 g). As shown in Figure 1 h, the Barrett–Joyner–Halenda (BJH) pore size distribution curves suggest that the three porous structures possess relatively uniform pores with average diameters of 2.3, 2.6, and 3.5 nm. Although the calculated average pore sizes of samples NCC1 and NCC2 do not differ significantly, it is apparent that NCC2 displays a broader size distribution and contains more relatively large pores with diameters in the range 3–4 nm. Because of the random packing of TiO_2 nanorods, the pore sizes of sample NCC3 are much larger than those of the other two clusters, which is consistent with the TEM observations. The Brunauer–Emmett–Teller (BET) surface areas are 240, 324, and 441 $m^2 g^{-1}$ for the three porous samples, and 37 $m^2 g^{-1}$ for TiO_2 solid microspheres. The values for these clusters are relatively large compared to other recently reported TiO_2 porous structures, whose BET surface areas are typically around 100 $m^2 g^{-1}$.[14,38] Interestingly, the surface areas of the porous clusters increase with the size of the primary nanocrystals, which seems to be inconsistent with simple geometric considerations as well as with previous reports.[26] This result may be explained by the fusion of the nanocrystals during calcination: smaller nanocrystals, which have larger contact area with neighboring particles and higher surface energy, are easier to fuse together at high temperatures, consequently leading to smaller specific surface areas.

Two approaches were used to evaluate the efficiency of the adsorption of phosphorylated proteins by as-obtained TiO_2 clusters (Scheme 1 b). One was measuring the difference of protein concentrations in the supernatant before and after adsorption; the other was directly measuring the protein concentration in the elution fraction. Specifically, the TiO_2 clusters were added to a protein mixture containing β-casein, horseradish peroxidase, and β-lactoglobulin (each 0.75 $mg mL^{-1}$) for 2 h. The mixture was subjected to centrifugation, and the supernatant was analyzed by capillary electrophoresis (CE) with UV detection at 200 nm; the precipitate was washed with washing buffer (50 % acetonitrile, 0.1 % trifluoroacetic acid) twice and subsequently eluted with aqueous ammonia (10 %). The eluent was collected and also analyzed by CE. In this example, only β-casein is a phosphate-containing protein. From the adsorption isotherm curve (see the Supporting Information), the equilibrium adsorption of β-casein by NCC1 can be reached in about 1 h even with a pore size of around 2.3 nm.

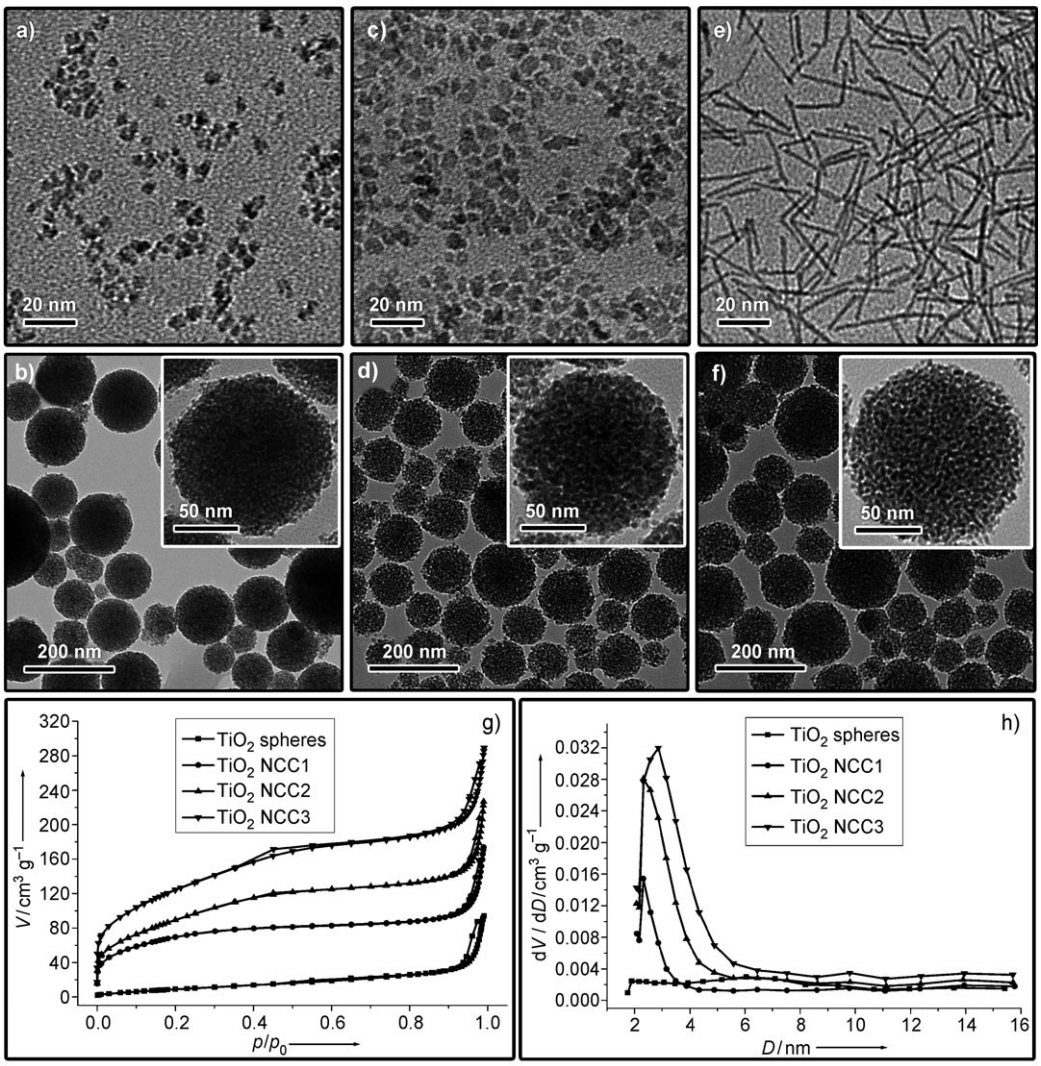

Figure 1. a–f) TEM images of TiO_2 nanocrystals and corresponding clusters assembled from the nanocrystals: a,b) NCC1; c,d) NCC2; and e,f) NCC3. Insets show TEM images at high magnification. g) N_2 adsorption–desorption isotherm curves for a sample of TiO_2 solid spheres and three samples of TiO_2 mesoporous clusters. *V*: volume, *p*: pressure of N_2. h) BJH pore size distribution curves for different TiO_2 materials. *D*: pore diameter.

Figure 2a,b shows the CE results by comparing the protein concentrations in the supernatant. The migration times of peroxidase, β-casein, and β-lactoglobulin are 2.6, 3.1, and 3.5 min, respectively. For the different materials, ranging from solid TiO_2 spheres to NCC1, NCC2, and NCC3, the peak area of β-casein decreases significantly. The corresponding adsorption efficiencies (the peak area decrease after enrichment relative to the peak area before enrichment) of β-casein by these four structures are 6.5%, 30.7%, 47.6%, and 62.4%. In contrast, the peak areas from peroxidase and β-lactoglobulin vary little after adsorption; less than 10% of these proteins were adsorbed by TiO_2 materials. The protein-loaded TiO_2 structures were washed with washing buffer and then eluted with aqueous ammonia. Figure 2c,d shows the CE results of the elution. It is clear that no peak of peroxidase (at around 2.6 min) or β-lactoglobulin (at around 3.5 min) is observed, and only β-casein can be detected. The strong peak at 2.3 min can be attributed to ammonia adsorption at 200 nm. TiO_2 NCC3 still shows the strongest adsorption for β-casein, which is consistent with the above results. The recovery efficiencies after washing and elution (the peak area after enrichment relative to that before enrichment) for β-casein can reach around 50% for the three porous TiO_2 clusters. In contrast, TiO_2 solid spheres cannot retain any β-casein after two washings, suggesting that the superior phosphorylated protein adsorption property of TiO_2 clusters may result from not only the affinity of the TiO_2 surface, but also the trapping effect of the mesoscale pores.

To test the size-exclusion effect of the pores, we used a mixture of two phosphorylated proteins with different molecular weights, β-casein (MW: 24 kDa) and fetuin (MW: 48 kDa). As shown in Figure 3a, the peak area of β-casein decreases significantly after adsorption onto TiO_2 materials. In particular, the adsorption efficiency of β-casein by NCC3 was calculated from the CE results to be 52.9% from the supernatant and 25.8% from the eluted fraction. Because the molecular weight of fetuin is about twice that of β-casein, it is more difficult for fetuin to pass through the pores with sizes of 2–3 nm. Therefore, the amount of fetuin in the supernatant does not decrease much after adsorption by TiO_2 clusters (Figure 3a), whereas only about 6% of the fetuin was eluted after washing (Figure 3c,d). The adsorption of fetuin is believed to be limited to the near surface regions of the clusters. From a comparison of the adsorption efficiencies for the two proteins, it is clear that β-casein can be selectively adsorbed in the pores of the clusters, whereas fetuin is essentially excluded.

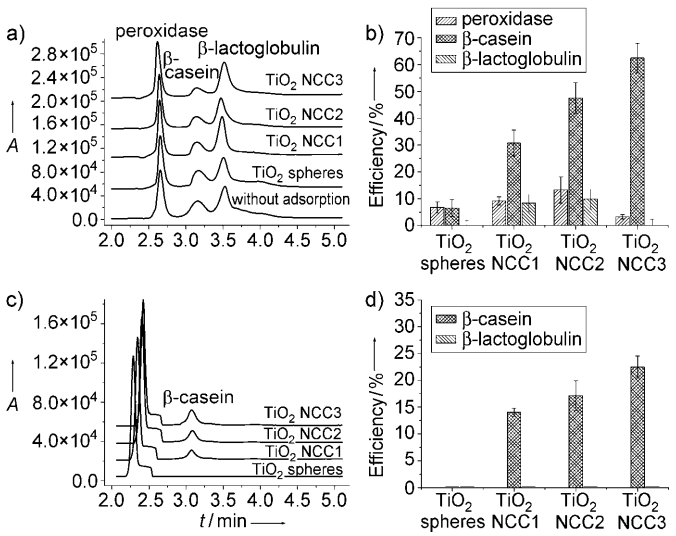

Figure 2. a,c) Electropherograms of the protein mixture studied: a) supernatant and c) eluent after enrichment by TiO_2 materials for 2 h. b,d) Corresponding adsorption efficiencies for proteins enriched by different TiO_2 materials.

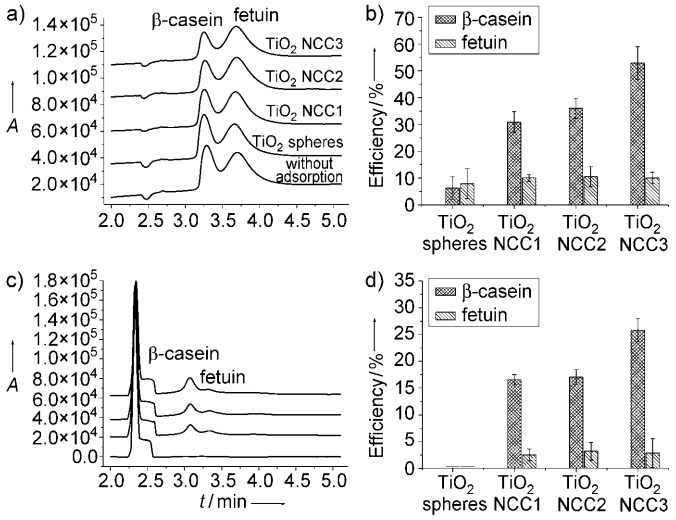

Figure 3. a,c) Electropherograms of the mixture of β-casein and fetuin: a) supernatant and c) eluent after enrichment by TiO_2 materials for 2 h. b,d) Corresponding adsorption efficiencies for the two proteins enriched by different TiO_2 materials.

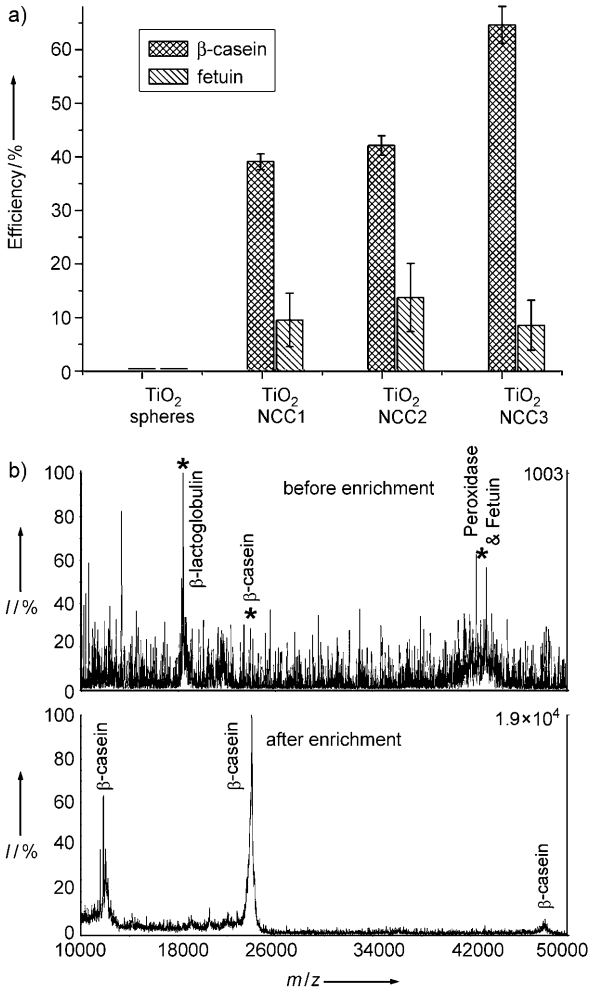

Figure 4. a) Comparison of enrichment efficiencies of phosphorylated proteins by different TiO_2 materials from a mixture containing low concentrations of β-casein, horseradish peroxidase, β-lactoglobulin, and fetuin. b) MALDI–TOF mass spectra of the protein mixture before and after enrichment by porous TiO_2 NCC3. Asterisks mark the peaks of the different proteins where they could be detected.

We also demonstrated the separation power of the TiO_2 nanocrystal clusters for low-concentration proteins. In actual applications, it is in fact a significant challenge to enrich low-abundance specific proteins in complex biological samples. A diluted protein mixture (β-casein, peroxidase, β-lactoglobulin, and fetuin, 0.01 $mg\,mL^{-1}$) was incubated with TiO_2 materials for 2 h. CE and MALDI–TOF MS analysis were performed to analyze the eluted fraction to evaluate the enrichment efficiencies of the phosphorylated proteins. The CE analysis (Figure 4a) shows enrichment efficiencies of β-casein by TiO_2 porous structures are 38.1%, 41.7%, and 64.1% for the three clusters, respectively (see the corresponding electropherograms in the Supporting Information). Nonporous TiO_2 spheres still cannot retain any phosphorylated proteins after being washed twice. The enrichment efficiencies for fetuin are much lower because of the size-exclusion effect, and no peroxidase and β-lactoglobulin can be detected in the eluted fraction because of the lack of specific affinity.

Figure 4b shows the MALDI–TOF mass spectra of the protein mixture before and after being treated by TiO_2 NCC3, from which a high selectivity for enrichment of β-casein is obvious. When the mixture was analyzed directly without enrichment, the signal of β-casein was extremely poor and only peaks for β-lactoglobulin could be identified with a low signal/noise (S/N) ratio. After selective enrichment, β-casein could be easily detected with a strong intensity and a high S/N ratio. Combining size exclusion with high specific affinity, the mesoporous TiO_2 clusters hold great potential for the selective enrichment of phosphorylated proteins from complex biological samples.

In summary, we have developed a general bottom-up assembly route to prepare porous nanocrystal clusters with

specific surface affinity for biomolecules. The size and surface chemistry of the pores can be conveniently controlled by changing the properties of the building blocks during assembly. The demonstrated example of porous TiO_2 nanocrystal cluster structures shows ideal properties for the selective enrichment of phosphorylated proteins or phosphopeptides: 1) They can be dispersed stably in water. 2) Their large specific surface areas ensure a high capacity for capturing the target molecules. 3) Because of the relatively large size of the clusters, they can be conveniently separated from the mixture by centrifugation. 4) The affinity of the TiO_2 surface for phosphate groups ensures the specific enrichment of biomolecules such as phosphorylated proteins and phosphopeptides. Elution can be easily performed by destroying the specific affinity using an alkaline solution. 5) The pore sizes are narrowly distributed and conveniently adjustable, promoting selective adsorption of proteins based on the size-exclusion mechanism. With all of these features, the porous TiO_2 clusters can effectively and selectively enrich low concentrations of intact phosphorylated proteins from protein mixtures. It is expected that the selective enrichment is not limited to phosphorylated proteins, but can also be extended to phosphate-containing peptides and DNA molecules. By appropriately selecting the oxide nanocrystals and their size and shape, this self-assembly strategy opens the door to a new class of mesoporous materials that may have wide applications in isolating biomolecules, in particular, low-abundance proteomic biomarkers. Our preliminary results also suggest that it is possible to incorporate multiple components into the clusters to enable many additional functions beyond enrichment.

Received: November 25, 2009
Published online: February 12, 2010

Keywords: mesoporous materials · nanoparticles · proteins · self-assembly · titanium

[1] R. Tian, M. Ye, L. Hu, X. Li, H. Zou, *J. Sep. Sci.* **2007**, *30*, 2204.
[2] Y. J. Han, G. D. Stucky, A. Butler, *J. Am. Chem. Soc.* **1999**, *121*, 9897.
[3] R. Terracciano, L. Pasqua, F. F. Casadonte, M. S. Preiano, D. Falcone, R. Savino, *Bioconjugate Chem.* **2009**, *20*, 913.
[4] T. Rosa, G. Marco, T. Flaviano, P. Luigi, T. Pierosandro, C. M. Ming-Cheng, A. J. Nijdam, F. P. Emanuel, A. L. Lance, C. Giovanni, F. Mauro, V. Salvatore, *Proteomics* **2006**, *6*, 3243.
[5] H. H. P. Yiu, C. H. Botting, N. P. Botting, P. A. Wright, *Phys. Chem. Chem. Phys.* **2001**, *3*, 2983.
[6] M. Hartmann, *Chem. Mater.* **2005**, *17*, 4577.
[7] A. Katiyar, L. Ji, P. G. Smirniotis, N. G. Pinto, *Microporous Mesoporous Mater.* **2005**, *80*, 311.
[8] A. Katiyar, N. G. Pinto, *Small* **2006**, *2*, 644.
[9] R. J. Tian, H. Zhang, M. L. Ye, X. G. Jiang, L. H. Hu, X. Li, X. H. Bao, H. F. Zou, *Angew. Chem.* **2007**, *119*, 980; *Angew. Chem. Int. Ed.* **2007**, *46*, 962.
[10] P. T. Tanev, T. J. Pinnavaia, *Science* **1995**, *267*, 865.
[11] R. Tian, L. Ren, H. Ma, X. Li, L. Hu, M. Ye, R. A. Wu, Z. Tian, Z. Liu, H. Zou, *J. Chromatogr. A* **2009**, *1216*, 1270.
[12] C. T. Kresge, M. E. Leonowicz, W. J. Roth, J. C. Vartuli, J. S. Beck, *Nature* **1992**, *359*, 710.
[13] M. E. Davis, *Nature* **2002**, *417*, 813.
[14] D. Chen, F. Huang, Y.-B. Cheng, R. A. Caruso, *Adv. Mater.* **2009**, *21*, 2206.
[15] D. Zhao, J. Feng, Q. Huo, N. Melosh, G. H. Fredrickson, B. F. Chmelka, G. D. Stucky, *Science* **1998**, *279*, 548.
[16] J. Tang, Y. Wu, E. W. McFarland, G. D. Stucky, *Chem. Commun.* **2004**, 1670.
[17] N. Phonthammachaia, M. Rumruangwonga, E. Gularib, A. M. Jamiesonc, S. Jitkarnkaa, S. Wongkasemjita, *Colloids Surf. A* **2004**, *247*, 61.
[18] Y. K. Hwang, Y.-U. Kwon, K.-C. Lee, *Chem. Commun.* **2001**, 1738.
[19] Y. Yin, A. P. Alivisatos, *Nature* **2005**, *437*, 664.
[20] A. R. Tao, S. Habas, P. Yang, *Small* **2008**, *4*, 310.
[21] B. Wiley, Y. Sun, J. Chen, H. Cang, Z.-Y. Li, X. Li, Y. Xia, *MRS Bull.* **2005**, *30*, 356.
[22] S. G. Kwon, T. Hyeon, *Acc. Chem. Res.* **2008**, *41*, 1696.
[23] Y. Li, X. Q. Xu, D. W. Qi, C. H. Deng, P. Y. Yang, X. M. Zhang, *J. Proteome Res.* **2008**, *7*, 2526.
[24] Y. H. Zhang, X. Y. Wang, W. Shan, B. Y. Wu, H. Z. Fan, X. J. Yu, Y. Tang, P. Y. Yang, *Angew. Chem.* **2005**, *117*, 621; *Angew. Chem. Int. Ed.* **2005**, *44*, 615.
[25] R. Klajn, K. J. M. Bishop, M. Fialkowski, M. Paszewski, C. J. Campbell, T. P. Gray, B. A. Grzybowski, *Science* **2007**, *316*, 261.
[26] D. S. Wang, T. Xie, Q. Peng, Y. D. Li, *J. Am. Chem. Soc.* **2008**, *130*, 4016.
[27] T. Hunter, *Cell* **2000**, *100*, 113.
[28] M. Mann, O. N. Jensen, *Nat. Biotechnol.* **2003**, *21*, 255.
[29] L. H. Hu, H. J. Zhou, Y. H. Li, S. T. Sun, L. H. Guo, M. L. Ye, X. F. Tian, J. R. Gu, S. L. Yang, H. F. Zou, *Anal. Chem.* **2009**, *81*, 94.
[30] S. Feng, M. L. Ye, H. J. Zhou, X. G. Jiang, X. N. Jiang, H. F. Zou, B. L. Gong, *Mol. Cell. Proteomics* **2007**, *6*, 1656.
[31] M. Mazanek, G. Mituloviae, F. Herzog, C. Stingl, J. R. A. Hutchins, J. M. Peters, K. Mechtler, *Nat. Protoc.* **2007**, *2*, 1059.
[32] G. T. Cantin, T. R. Shock, S. K. Park, H. D. Madhani, J. R. Yates, *Anal. Chem.* **2007**, *79*, 4666.
[33] M. Rainer, H. Sonderegger, R. Bakry, C. W. Huck, S. Morandell, L. A. Huber, D. T. Gjerde, G. K. Bonn, *Proteomics* **2008**, *8*, 4593.
[34] A. Dubrovska, S. Souchelnytskyi, *Proteomics* **2005**, *5*, 4678.
[35] G. C. Adam, E. J. Sorensen, B. F. Cravatt, *Mol. Cell. Proteomics* **2002**, *1*, 781.
[36] F. Bai, D. S. Wang, Z. Y. Huo, W. Chen, L. P. Liu, X. Liang, C. Chen, X. Wang, Q. Peng, Y. D. Li, *Angew. Chem.* **2007**, *119*, 6770; *Angew. Chem. Int. Ed.* **2007**, *46*, 6650.
[37] J. Ge, Y. Yin, *Adv. Mater.* **2008**, *20*, 3485.
[38] Y. J. Kim, M. H. Lee, H. J. Kim, G. Lim, Y. S. Choi, N.-G. Park, K. Kim, W. I. Lee, *Adv. Mater.* **2009**, *21*, 3668.

